CHAPTER 2

EXPERIMENTAL

Two experimental techniques have been employed in this thesis for determining bubble behavior such as bubble size distribution, bubble velocity and local gas holdup in a bubble column. These are the five-point electrical conductivity probe technique and the dynamic gas disengagement technique. The dynamic gas disengagement technique will be described in Chapter 7. This chapter only describes the experimental apparatus used and the basic principles behind the five-point conductivity probe technique.

The main experimental purposes (using the five point conductivity technique) are to understand bubble behavior in bubble columns, to verify modeling work and to determine model parameters. Hence, not all measured results are shown in this chapter, except those involved in this thesis.

2.1 Experimental Apparatus

All the experimental work in this thesis has been carried out in a plexiglass column with inner diameter 0.288 m and height 4.33 m, as shown in Figure 2.1. The gas distributor was placed between the main column section and a stainless inlet section. The distributor plate had 250 holes (1 mm inner diameter) for gas and 19 holes (28 mm inner diameter) for liquid. Clean compressed air was fed

to the column from a pipeline air source with stabilized pressure. A personal computer was used to measure, record and store temperatures (T) and flow rates (F) in experimental processes. The measurement of pressure (P) was done by pressure gauges.

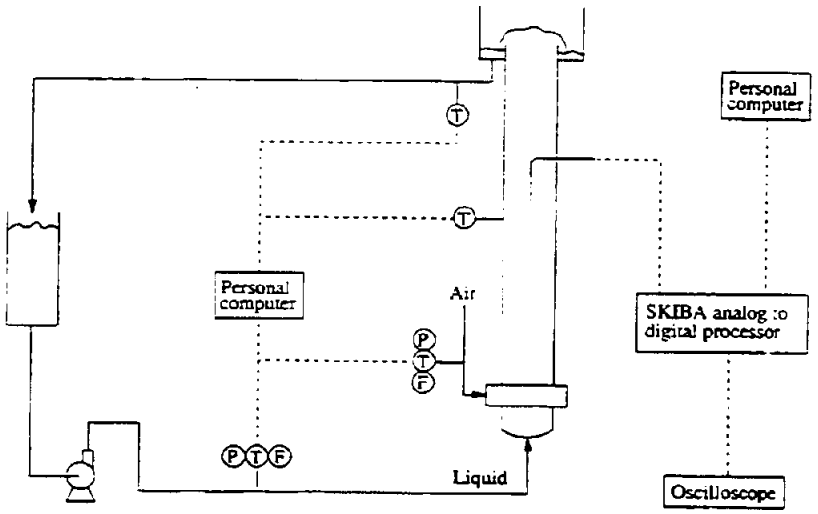

Figure 2.1 Sketch of experimental apparatus.

The bubble size and rise velocity were measured by a five-point conductivity micro-probe with the tip diameter ~0.3 mm connected to a signal processing unit system. The system, which is commercial (SKIBA LMSN-5), consists of a real time signal recording and storage unit connected via an interface card to a personal computer. An oscilloscope was used to calibrate the conductivity probe.

Measurements of bubble behavior using the five-point conductivity probe technique were done only for the air-water system. The superficial gas and liquid velocities were varied in the ranges, 0.02-0.2 and 0-0.02 m/s, respectively. The temperatures used were 11±1 °C and 25±1 °C.

Measurements were made at two levels along the column height, at distances 0.2 and 2.0 m from the gas distributor respectively. For each level, measurements were made at several radial positions corresponding to the following values of dimensionless radius: 0 (at the center), 0.25, 0.5, 0.6, 0.7, 0.8, 0.9 and 0.95.

2.2 Measurement Principle

The conductivity probe technique utilizes the difference in electrical conductivity between the liquid and the gas phases. When the probe sensor encounters a bubble in the liquid, a square pulse of voltage is generated. The conductivity technique was early used for determining local gas void fractions with a one-point (sensor) probe and was later developed to also measure bubble sizes, bubble velocities and bubble frequencies.

However, in order to measure bubble behavior such as bubble size distribution and bubble motion, a conductivity probe needs at least two sensors. The two-point conductivity probe has two sensors and has been frequently used (Buchholz, 1981; Yu and Kim, 1990). However, the two-point conductivity probe has a low accuracy and can only give bubble chord lengths, and not bubble volume or equivalent diameter. In order to enable determination of bubble curvature and thereby bubble volume, probe techniques with more points have been developed.

2.2.1 The five-point probe of Burgess and Calderbank

The five-point conductivity probe technique was first developed by Burgess and Calderbank (1975). The probe has five conductivity sensors with spatial orientation as sketched in Figure 2.2. This probe was connected to a digital computer (Burgess and Calderbank, 1975).

When a bubble approaches the probe sensor assembly, a voltage pulse sequence will be generated. A schematic diagram of a typical sequence is shown in

Figure 2.3, where T_i (i = 0, 1, 2, 3 and 4) indicates the bubble caused pulse duration time for probe sensor i, and t_i (i = 1, 2, 3 and 4) is the response delay time for probe sensor i relative to probe sensor 0.

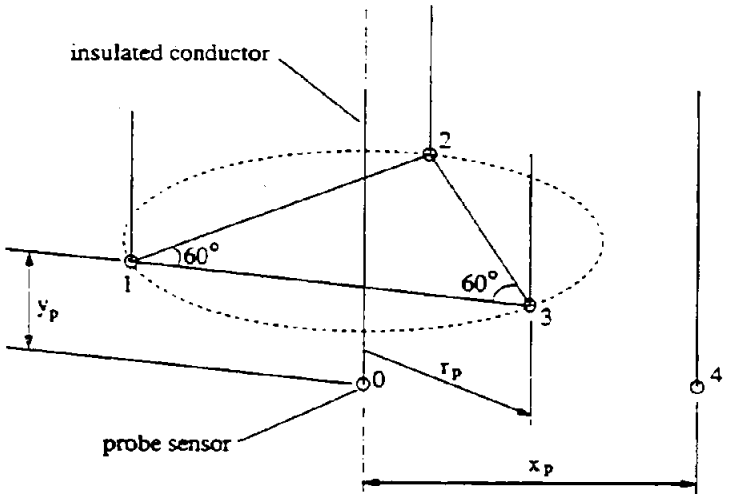

Figure 2.2 Spatial orientation of the probe tips developed by Burgess and Calderbank (1975).

The main advantages of this five-point technique are as follows.

(1) The probe is capable of resolving the position at which it is struck by the bubble relative to the bubble central line. In other words, it can distinguish whether the encountered bubbles are symmetrical around the probe axis (probe sensor 0). It will accept small deviations from symmetry and record all the accepted bubbles. For description convenience, in what follows, the measured bubbles being approximately symmetrical with the probe axis are termed "true bubbles", otherwise "false bubbles".

(2) The instance the probe sensor enters a true bubble can be relatively accurately determined. One has to bear in mind that in liquids the probe will be wet and

the film drainage time can result in a significant departure from a step change in voltage.

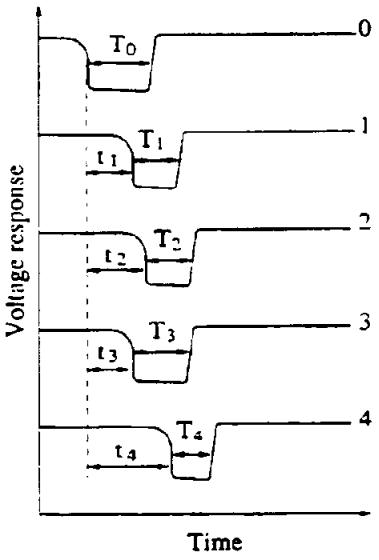

Figure 2.3 Sketch of pulse sequence.

(3) For the true bubbles recorded, accurate rise velocities may be obtained. The shape of a true bubble can be inferred from the different signal lengths generated by different probe sensors, as seen in following discussion. Hence, the bubble volume may be estimated with good accurately, especially when compared to the two-point probe technique.

However, since most of the bubbles encountered by the probe may not be symmetrical around the probe axis, a large number of bubbles will be wasted using this technique. In addition, the bubble rise velocities obtained by this technique for "true bubbles" may be seriously in error. This is because the technique assumes vertically rising bubbles, whereas the registered bubbles will probably have a more randomly distributed direction (see later).

2.2.2 The five-point probe of Steinemann and Buchholz

A great improvement in the five-point conductivity probe technique was made by Steinemann and Buchholz (1984). They proposed a similar design to that of Burgess and Calderbank (1975). The difference in design is only that the 4th probe sensor is placed at the same radial position as the 1-3rd sensors, as shown in Figure 2.4.

Based on this design, Steinemann and Buchholz (1984) developed the estimation methods for determining not only bubble size distribution, bubble velocity and frequency of bubbles, but also direction of bubble motion, through analyzing the

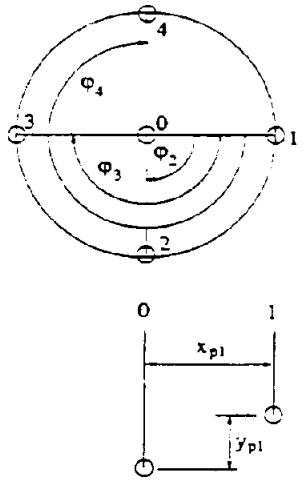

Figure 2.4 Probe design of Steinemann and Buchholz (1984).

recorded voltage pulse sequence like Figure 2.3. This technique does not reject the recorded bubbles that are not symmetrical around the probe axis, but utilizes all the recorded information as much as possible. The direction of bubble motion can be estimated by using the principles of analytical geometry. However, the estimation methods are complicated and may induce large errors when the bubble shape departs significantly from a sphere or an ellipsoid.

This technique has been used in the SKIBA LMSN-5 system.

2.3 Estimation of the Bubble Parameters

2.3.1 Technique of Burgess and Calderbank

Although the five-point conductivity probe technique suggested by Burgess and Calderbank (1975) has not been used by this work, its estimation methods for bubble velocities and sizes are given as follows, in order to understand, what are and why it has, the disadvantages.

For a measured true bubble, which is symmetrical around the probe axis (at probe sensor 0 in Figure 2.2), the bubble rise velocity can be calculated by

$$u_{b,z} = \frac{3y_p}{t_1 + t_2 + t_3} \tag{2.1}$$

where y_p is the probe separation as defined as in Figure 2.2 and is accurately known. This estimation method is based on the assumption that the true bubbles always move vertically upwards. If this is true, the estimation method is quite accurate. However, if a bubble moves at an angle to the vertical, the estimated bubble rise velocity may be in a large error.

The central vertical chord length for the true bubble, L_c, can then be obtained by

$$L_c = u_{b,z} T_0^m \tag{2.2}$$

where T_i^m (here $i = 0$) is the modified pulse duration time for probe sensor i (Burgess and Calderbank, 1975) and was considered to represent the real pulse duration time by the authors.

Probe sensor 4 is used to measure the vertical distance, L_d, between the bubble leading surface at the centerline and at the radial position, x_p. It also measures the bubble vertical length at this position, L_e. Accordingly,

$$L_d = u_{b,z} t_4 \tag{2.3}$$

and

$$L_e = u_{b,z} T_4^m \tag{2.4}$$

The bubble volume may relatively accurately be estimated from the parameters, L_c, L_d, L_e and x_p, according to known correlations that are available (Tadaki and Maeda, 1961; Clift *et al.*, 1978; Fan and Tsuchiya, 1990).

For the measurement of local gas holdup, only the signals of the central sensor are used, similar to the one-point conductivity probe technique. This gives

$$\varepsilon_G = \frac{\sum T_0^m}{t_{total}} \tag{2.5}$$

where Σ indicates the sum of all responses, including both true and false bubbles, encountered by the central sensor within a given measurement period t_{total}.

2.3.2 Technique of Steinemann and Buchholz

For a meaningful interpretation of the signal combinations using the design of Steinemann and Buchholz (1984), one has to describe the complete bubble motion including the absolute bubble velocity, $u_{b,a}$, the angle between the probe axis and the bubble trajectory (vertical angle), θ, and the horizontal angle, φ, as defined in Figure 2.5. For vertically ascending or descending bubbles, θ will be zero or 180° respectively. The horizontal angle, φ, takes values 0-360° and gives information about the direction of bubble motion. For an estimation of the parameters, $u_{b,a}$, θ and φ, a nonlinear system of equations combining the probe signals with the parameters of the probe geometry (see Figure 2.4) must be solved.

The estimation equations for the three parameters, $u_{b,a}$, θ and φ, have been given by Steinemann and Buchholz (1984) as follow

$$u_{b,a} = \frac{2y_{pi}^{m}}{T_0 + T_i}, \quad i = 1,2,3,4 \tag{2.6}$$

where

$$y_{pi}^{m} = y_{pi}\cos\theta - x_{pi}\sin(\varphi + \varphi_i)\sin\theta \tag{2.7}$$

It is found that there are four equations for the three unknown parameters $u_{b,a}$, θ and φ. Thus, the over-determined system of equations can be solved by minimization. The over-determination of the system of equations compensates for possible errors introduced by the determination of the pulse time (Steinemann and Buchholz, 1984).

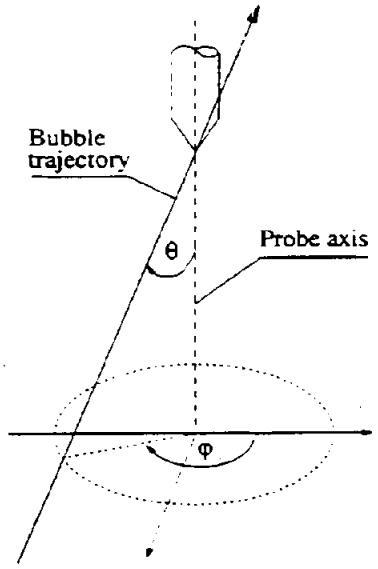

Figure 2.5 Definition of Bubble movement parameters.

With the known three parameters of bubble motion, it is possible to estimate the coordinates of the bubble surface from the probe signals and the probe geometry. To do this, Steinemann and Buchholz (1984) has given a complex correlation, assuming the bubbles to be spheres or ellipsoids of rotation. The bubble size can then be estimated from the coordinates of the bubble surface.

As seen, this technique does not need to assume bubble rising vertically. The bubble rise velocity can be calculated from the absolute bubble velocity, $u_{b,a}$ and the vertical angle, θ. Hence, it is generally more accurate than that obtained by the technique of Burgess and Calderbank (1984).

However, this estimation is complicated and needs solving another system of equations (Steinemann and Buchholz, 1984). Hence, the computation time on a personal computer for a measurement is usually long. In addition, as mentioned before, this technique may induce large errors when the bubble shape departs significantly from a sphere or an ellipsoid.

The measurement of local gas holdup is done in the same way as by the technique of Burgess and Calderbank (1975) or by the one-point conductivity probe technique, as expressed by Equation (2.5).

2.4 Experimental Results

Figure 2.6 Shows the examples of local bubble size distributions measured by the five-point conductivity probe technique. It is seen that the small bubbles have

higher number percentage but usually lower volume percentage. There clearly are more large bubbles in the column center. In the zone near the wall, it can be found more small bubbles than in the central zone and nearly no bubbles larger than about 15 mm. However, higher volume percentages for bubbles in the size range about 10-15 mm in the zone close to the wall can still be found. This is mainly caused by the strong liquid circulation at the gas velocity (u_G = 10 cm/s).

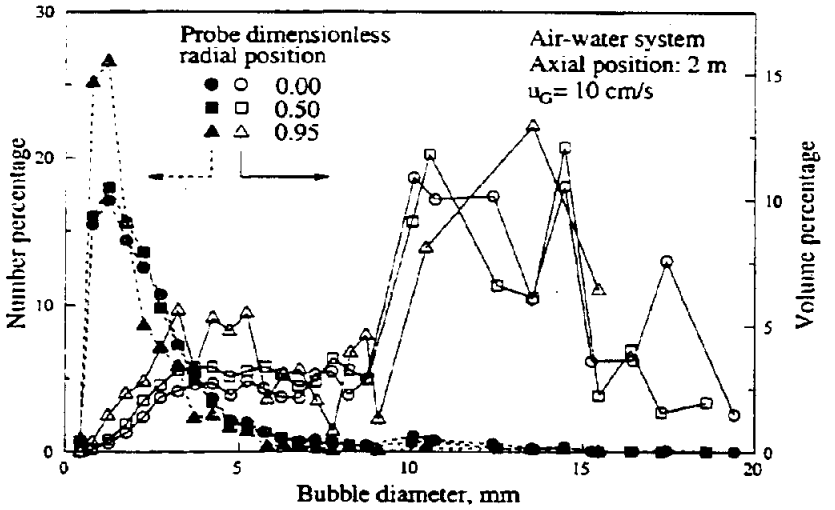

Figure 2.6 Local bubble size distributions at u_G = 10 cm/s, measured by the five-point conductivity probe technique.

Figure 2.7 shows the averaged bubble size distributions over the cross-section area at various superficial gas velocities. It is found that usually the lower the gas velocity, the more the small bubbles. At superficial velocities lower than 6 cm/s, nearly no bubbles larger than about 15 mm exist and the bubble volume percentages for small bubbles are very close. This indicates that bubble size distributions at u_G < 6 cm/s changes little with superficial gas velocities (but bubble densities may change a lot). This flow regime, u_G < 6 cm/s, is termed the "homogeneous flow regime", as well known.

Comparing the curves at u_G = 6-10 cm/s in Figure 2.7, it can be found that the changes in bubble size distribution are significant. This is the so-called transition flow regime. There are much more large bubbles at u_G = 10 cm/s than those at u_G = 6 or 8 cm/s. This is because, for the coalescing system, the effect of bubble coalescence becomes strong, due to the bubble number densities are increased to a certain value when the gas velocity is increased to about 6 cm/s.

With increasing the gas velocity, effect of breakup becomes more and more important. At u_G > 10 cm/s (the heterogeneous flow regime), the bubble size distributions seem to become stable again. This may indicate that the system has achieved a fully turbulent condition at u_G > 10 cm/s.

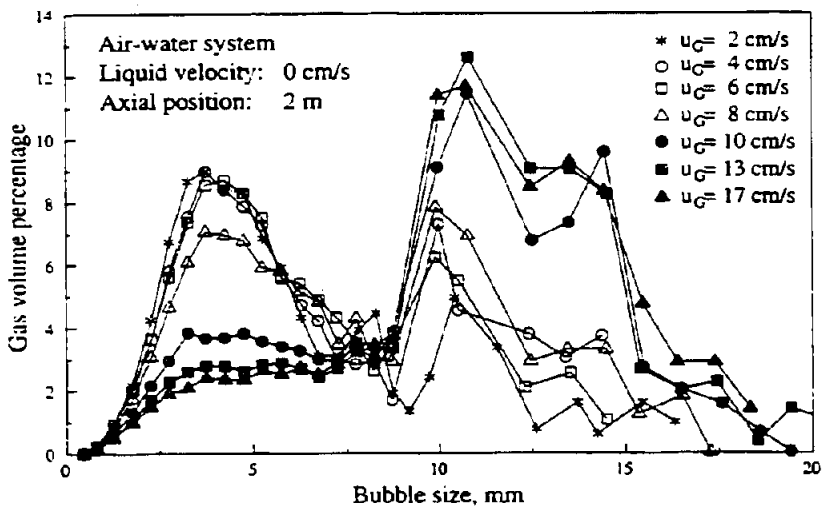

Figure 2.7 Bubble size distributions at various superficial gas velocities, measured by the five-point conductivity probe technique.

Measurement examples of the bubble parameters, $u_{b,a}$, θ and φ, as well as the local gas holdup by the five-point conductivity probe technique, are shown in Figure 2.8 - Figure 2.11. In all these examples, the superficial liquid velocity was zero.

Figure 2.8 shows that the larger the bubble size, the higher the absolute velocity of bubble motion. For a given bubble size, the absolute bubble velocity at the column center is usually higher than that close to the wall. This is because the liquid velocity at the center is higher.

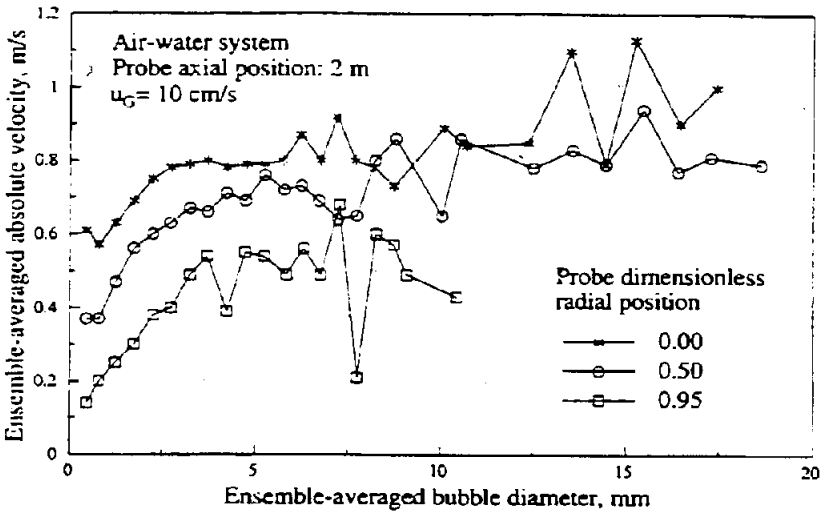

Figure 2.8 Absolute velocities of bubble motion, $u_{b,a}$, at u_G = 10 cm/s, measured by the five-point conductivity probe technique.

An estimate for the liquid velocity can be obtained by assuming that the smallest bubbles move with the liquid and have the same velocity as the liquid. In this way, it can be found, from Figure 2.8, that the slip velocities between bubble and liquid close to the wall are higher than those at the center. This can also be found in the experiment of Yao *et al.* (1991), where both bubble and liquid velocities were simultaneously measured. This is reasonable, because large bubbles are mainly concentrated in the central zone of a column and there exist a number of wakes generated by and moved with the bubbles (Crabtree and Bridgwater, 1971; Miyahara *et al.*, 1984, 1991). Small bubbles moving into the zone will be accelerated by the wakes and then have higher velocities. Hence,

the averaged velocity differences between the bubbles and the wakes or liquid (or the smallest bubbles) in the central zone will be smaller than those in the zone close to the wall.

It is noted that, for the measurement point close to the wall, nearly no bubbles larger than about 11 mm are registered. This means that there are less large bubbles close to the wall due to the effect of liquid circulation. Large bubbles tend to concentrate in the central part.

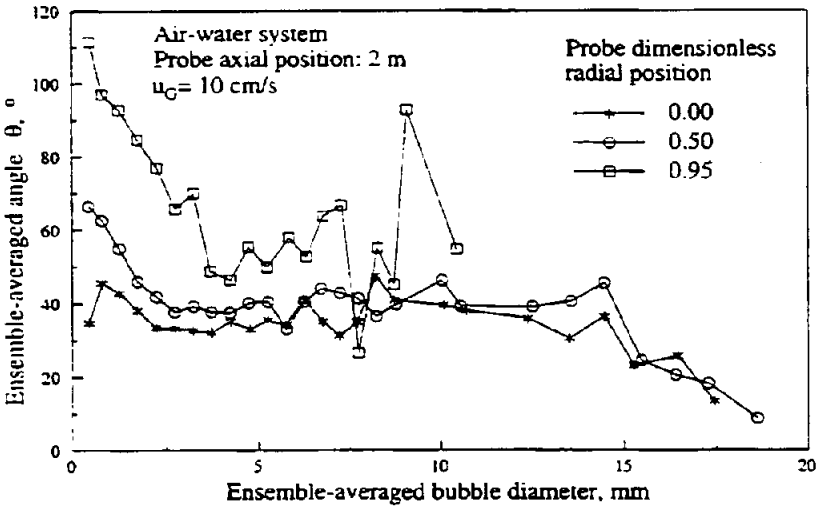

Figure 2.9 Vertical angles of bubble motion, θ, at u_G = 10 cm/s, measured by the five-point conductivity probe technique.

Figure 2.9 shows the ensemble-averaged angles between the probe axis and the bubble trajectory, θ. For the measurement point at the column center, it is found that the deviations from verticality for bubbles larger than about 2.5 mm are between 0-80°, since the averaged values are about 40°. For the bubbles smaller than 2.5 mm, the deviation angles may be between 0-90°. This indicates that a large portion of the bubbles passing the probe move upward non-vertically. However, the bubbles larger than about 15 mm show a more vertical movement

($\theta \approx 0$-40°). This is reasonable, since the larger the bubble size, the stronger the effect of buoyancy.

For the measurement point at the dimensionless radial position 0.5, the bubble movement seems more seriously out of the vertical, especially for small bubbles. For the position close to the wall, it is seen that part of the bubbles are clearly in downward movement, especially for bubble sizes lower than about 3 mm.

From Figure 2.10, the predominant directions of bubble motion in a horizontal plane can be found . As seen from the figure, at the dimensionless radial positions of 0 and 0.5, the average horizontal angles are about 180° for bubble sizes smaller than about 15 mm. This value means that the horizontal angle, φ, may be randomly distributed in the range 0-360° and that the bubbles move towards the probe from any direction around the probe. No preferential direction can be detected. For bubble sizes larger than 15 mm it seems like the bubbles move towards the probe mainly from a certain side. This result may also be caused by measurement errors since a smaller number of bubbles above 15 mm were recorded. However, for the radial position close to the wall, most of the bubbles have a certain preferential probe approach direction. The non-randomness of the approach is statistically significant.

The local gas holdups measured by the probe technique at various superficial gas velocities are shown in Figure 2.11. When the profiles are integrated over the cross-section and compared with the simultaneously measured overall gas holdups, which are shown in Figure 2.12, it was found that the results measured by the conductivity probe were consistently on the low side. Menzel (1989) also concluded that the gas holdups obtained by the probe technique were about 20% lower than those measured by the pressure difference method. There may be many reasons for this discrepancy. For instance, the probe cannot measure bubbles smaller than, or equal to, the probe tip (about 0.3 mm), the probe rod may affect bubbles moving from the upper position to the probe tip and so on. Another reason may be the axial variation of gas holdup.

From Figure 2.11 or Figure 2.12, it can be found that there is a clear transition in flow regime between about 6-10 cm/s of superficial gas velocity for the air-

water system. At a superficial gas velocity lower than about 6 cm/s, the overall gas holdup increases fast with increase in the gas velocity. This is because in this regime (the homogeneous flow regime), an increase in the gas velocity makes the bubble concentration increase, whereas the bubble size distribution changes little as shown in Figure 2.7. With a continuous increase in the gas velocity, the effect of coalescence becomes more significant and then more large bubbles are formed. Therefore, at the gas velocities above about 6 cm/s, the overall gas holdup goes down. At gas velocities higher than about 10 cm/s (the heterogeneous flow regime), the bubble size distribution has stabilized (see Figure 2.7) and overall gas holdup goes up again because of increased gas flow. Figure 2.11 also shows that the radial gas holdup distribution in heterogeneous flow regime is sharper than that in the homogeneous regime.

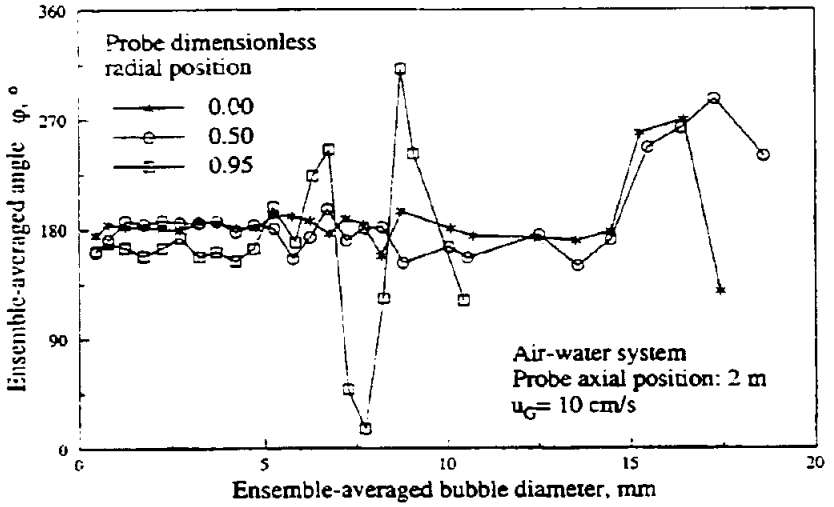

Figure 2.10 Horizontal angles of bubble motion, φ, at u_G = 10 cm/s, measured by the five-point conductivity probe technique.

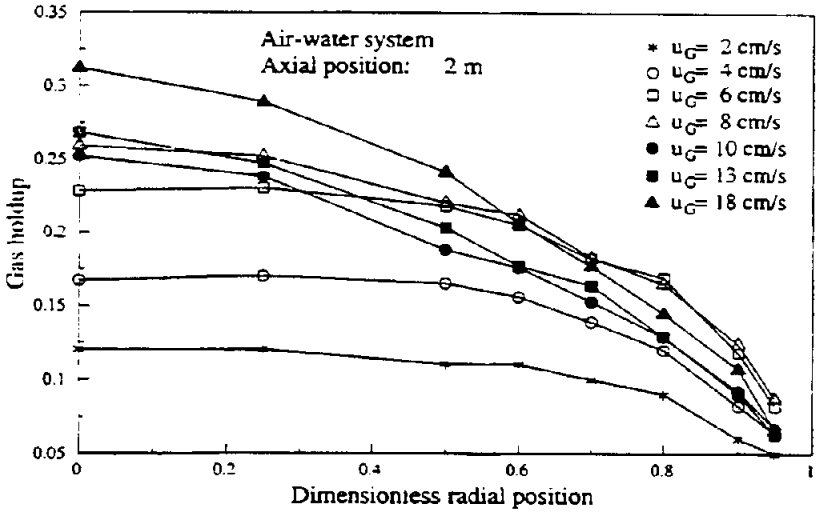

Figure 2.11 Local gas holdups at various superficial gas velocities, measured by the five-point conductivity probe technique.

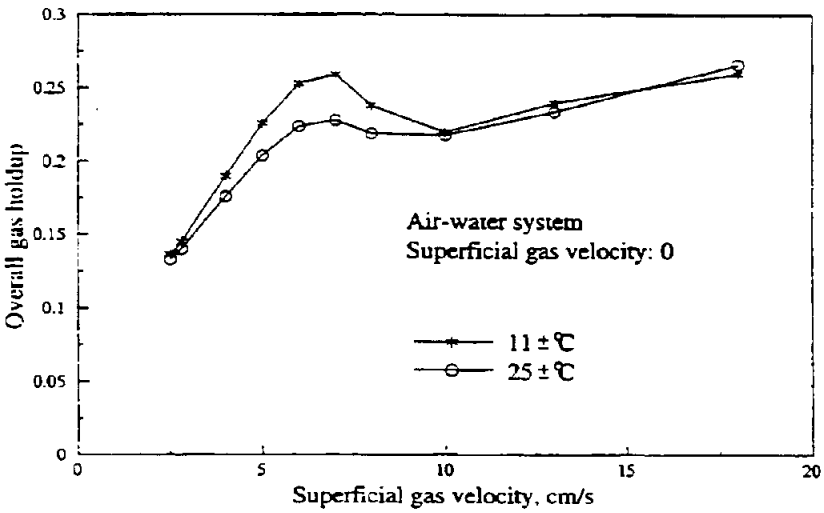

Figure 2.12 Overall gas holdups at various superficial gas velocities.

Also from Figure 2.12, it can be found that the overall gas holdups at 11 °C are usually larger that those at 25 °C, especially at low and intermediate superficial gas velocities. This may mainly be caused by the effect of liquid viscosity which is more significant for small bubbles. The viscosity of water at 11 °C is about 1.3 times as that at 25 °C. A higher liquid viscosity can usually make bubbles, chiefly small and intermediate bubbles, rise slower and make the residence time of bubbles in the liquid longer. At high gas velocities, this effect becomes weak due to more large bubbles formed.

2.5 Conclusion

The five-point conductivity probe technique can give a whole range of information such as bubble velocity, bubble size distribution, direction of bubble motion, bubble frequency and local gas holdup. It is very useful for understanding bubble behavior and for verifying modeling work. However, the five-point conductivity probe technique has some disadvantages. For example,

(1) It is limited to systems where the used liquid has a certain minimum electrical conductivity.

(2) The measured gas holdups are usually underestimated.

(3) The results are sensitive to the relationship between the bubble parameters, $u_{b,a}$, θ and φ and the bubble shape, which should be known and reliable. The relationship used by Steinemann and Buchholz (1984) is only suitable for bubbles of ellipsoid or spherical shapes. Estimated bubble sizes for bubbles shapes much different from spherical or ellipsoid may be seriously in error.

(4) Two non-linear systems of equations must be solved for each bubble in order to obtain the parameters for the bubble movement and shape. Hence, the computation time for a measurement is long.